Radio Interferometry: Theory, Techniques and Applications,
IAU Coll. 131, ASP Conference Series, Vol. 19, 1991,
T.J. Cornwell and R.A. Perley (eds.)

THE DESIGN OF HIGH FREQUENCY ANTENNAS

J.Delannoy
IRAM, 300 Rue de la Piscine, D.U. de GRENOBLE
38406, Saint Martin d'Heres - Cedex, FRANCE

ABSTRACT The conceptual guidelines in designing mm radio-telescope antennas are enlightened by some recent progress in their mechanical construction, and opto-radio-geometrical adjustment. This paper reviews concepts, illustrated in many existing solutions, including the new "phase-retrieval" holography for single dish adjustment (D.Morris, IRAM, 1982): 2 amplitude only maps at focus and out of focus, with enough dynamic range and signal to noise ratio, give surface errors within hours.

INTRODUCTION

The design of large antennas usable at mm or submm waves as radio-telescope's elements involves problems presented under 3 main headings:

(1) The surface accuracy, and the pointing accuracy, are compulsory targets. Structural calculations, pointing analysis, thermal model are key items in the design, in view of choices as astrodome or not, short focus limits, etc...

(2) Clean beams can be obtained with off-axis structures. The field-of-view versus aberrations trade-off becomes difficult at shorter waves: shapes and quality choice of reflecting surfaces require new efforts.

(3) Holography is renewing measurements techniques. Interferometry with an auxiliary antenna, close to working frequency, multiplexes sampled phase errors within the aperture plane, referenced to a plane wavefront from the point source. Without auxiliary antenna, the phase retrieval method uses 2 amplitude only maps, but needs more signal to noise.

THE "MUST'S": stigmatism, surface and pointing accuracies

To detect weak signals from remote sources in the Universe, proper use of large telescope surfaces and sensitive modern receivers must be achieved: in the mm range, SIS junctions cryogenic mixers plus cooled IF amplifiers are good "state of the art" representatives; bolometric detectors have advantages in wide-band work.

Monochromatic plane waves can describe noise signals with some care: spectral power density and phase randomness are the keys. Atmospheric perturbations are described in optics with speckles, in radio the "Fried parameter" -a coherence distance along wavefronts- suffices. One has to couple

with maximum efficiency the energy of a deterministic incoming plane wave to the receiver. The hybrid mode corrugated horn currently used as the wave collector at mm waves has a well defined center of phase. Maximum coupling to the single moded wave from collector to mixer is reachable with stigmatic surfaces, between infinity and the phase center, a geometry valid at all frequencies. One should provide a constant phase from any part of a plane wavefront to a focus, the phase center. From Fermat's principle the actual ray path is an extremum: should we slightly modify impact points on optical surfaces, then the optical path stays invariant to first order. This is a way to calculate pointing errors and aberrations in misaligned systems, starting from the geometrically stigmatic instrument. In emission, it sends a wave with plane equiphase surfaces, diffraction coming from aperture limitation with an angular Airy radius of $1.22\lambda/D$ radians (uniform illumination). D = diameter, illumination weight = modulus of E-field in aperture (each element of the aperture contributes to E sum, not power as measured in dB).

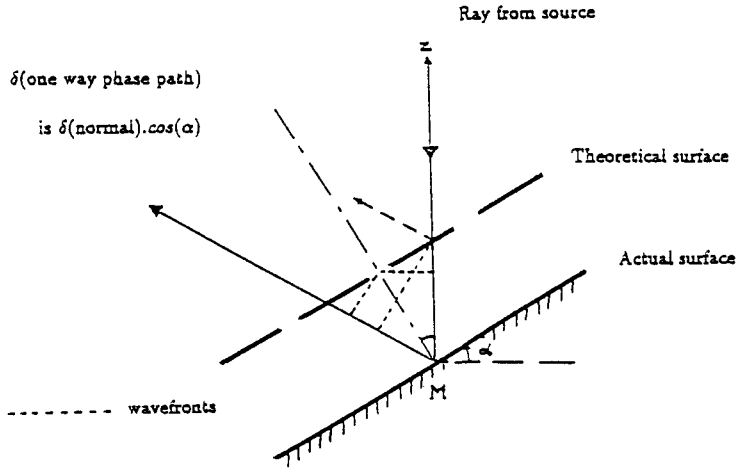

Figure 1: z error, normal error, phase error on a reflector.

Surface errors being dz along the pointed z direction, it is common practice to specify the $dz.\cos\alpha$ normal to surface if incidence angle is α. The one-way pathlength is then $\epsilon = dz.\cos^2\alpha$ (see fig. 1). This ϵ error perturbs at focus the ideal build-up of electrical field from a given direction and polarisation, summed from each area element in aperture with a phase $4\pi.\epsilon/\lambda$ (we have a reflector: double path; λ is the wavelength; see fig. 2). A gaussian distributed phase of equal moduli components gives a sum reduced by $\exp(-\sigma_\varphi^2/2)$: this on E-field, then we get on power $\exp(-\sigma_\varphi^2)$. This result was given by Ruze (1966) with a number of refinements. It is commonly used to specify surface accuracy at each wavelength within the range of existing designs, 1::3 or 1::10. If:

$$\exp(-\sigma_\varphi^2) = \exp[-(\frac{4\pi\sigma_\epsilon}{\lambda})^2] \qquad \text{with} \qquad \sigma_\epsilon = \frac{\lambda}{N} \qquad \sigma_\varphi = \frac{4\pi}{N}$$

then N gives the Ruze degradation. As N =15.1 means half efficiency, many designers take N =16 as a lower limit. A typical 50μ rms surface accuracy follows

https://doi.org/10.1017/S0252921100013002 Published online by Cambridge University Press

in the mm range: for more than 6 to 8m diameter, this exceeds the stiffness or thermal static limits (Von Hoerner 1967) of classical construction techniques. Sophistications are then used, including the passive homology principle, active aberration minimisation, passive pointing compensation, ventilation systems, new materials (as CFRP : Carbon Fiber Reinforced Plastic composites). CFRP has low thermal expansion, say 2 to 3 ppm/°C, less with cost. It has been used at IRAM and SEST in structures (Aspenas 1985), otherwise in panels (Japan 1980); the SMT (Martin, Baars 1990: MPIfR and TEXAS University submillimeter 10m antenna, 15μ rms) now under construction uses extensively CFRP components. Coming projects: the SMA (Mason 1990: SAO, 7 antennas 6m in diameter) and MMA (NRAO 1990: 40 antennas 8m in diameter) mm array projects are considering CFRP in supporting structure, associated to cast-alloy panels. For space telescopes (e.g. at ESA/ESTEC: 4.5m FIRST with 6μ rms, deployable 20m IVS for VLBI with 300μ rms, CFRP structures and panels are preferred by all potential contractors. Table 1 (updated from Baars) compiles the overall error budget of major facilities at mm waves.

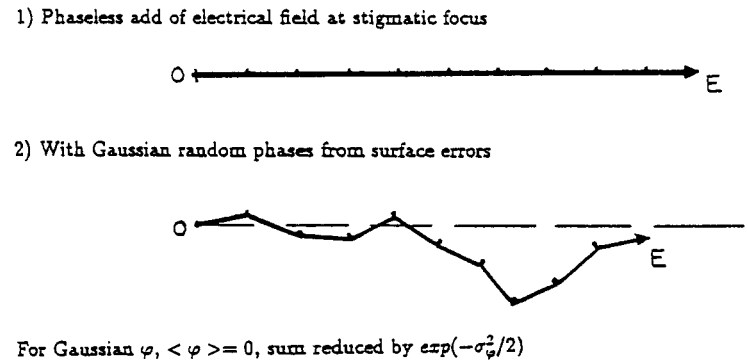

Figure 2: Surface errors and focal field build-up.

Pointing accuracy for mm antennas may be linked to phase variations over a diameter, as over the baseline in interferometric pointing. A $d\theta$ pointing error induces a linear phase error accross the aperture, reaching $\pm\pi D.d\theta/\lambda$ on a point source. An rms to be put into the Ruze exponent is $\pi D.d\theta/2\lambda$ for circular apertures, gain drop is $\exp(-\sigma_\varphi^2)$, as Ruze factor with $N = 8K$ in fig. 3. The current practice is to take one tenth (97.6% gain) or one twentieth (99.4%) of a main lobe: this pointing accuracy means 1 to few arc-seconds at mm waves on most existing telescopes, do not underestimate the corresponding mechanical challenge on large structures !

Some details of calculations carried out before building the IRAM 15m antennas are accessible in IRAM "WR" series, WR 205 summarizing main points here. The panel's size is dominated by thermal deformations in curvature: there is a wide consensus today to think that precision large reflectors must be built from smaller panels, independently supported, and corrected if needed (an evolved example with IR capabilities from 300 to 30μ in λ is the 10m, f/D =1.75, Keck telescope (U.C., Cal-Tech 1988) under construction, using capacitive sensors on the edge of 36 grinded hexagonal glass panels to maintain

TABLE 1: Major Telescopes for the millimeter wavelength range

INSTITUTE	LOCATION	HEIGHT (m)	YEAR	D (m)	RMS (1E-6m)	D/RMS (1E+03)	Lambda min. (mm)	MEASUREMENT METHOD
1. Max PLANCK Institut fur Radioastronomie (MPIfR)	Effelsberg, Germany	300	1983	100 75	500 350	200 215	6.3 4.4	theodolite, holography
2. Onsala Space Observatory	Onsala, Sweden	10	1976	20	180	110	2.3	theodolite, holography
3. Bell Laboratories	Crawford Hill, NJ, USA	115	1977	7	100	70	1.3	template
4. Univ. of Massachusetts	Amherst, MA, USA	300	1978	13.7	130	105	1.6	theodolite, holography
5. Calif. Inst. of Techn.	Owens Valley, CA, USA	1220	1979	10.4	40	260	0.5	laser (dist.), holography
6. Tokyo Observatory	Nobeyama, Japan	1350	1982	45	94	475	2.0	laser (theodol.), holography
7. Nat. Radio Astron. Obs.	Kitt Peak, AZ, USA	1940	1984	12	75	160	0.9	template, holography
8. MPIfR / IRAM	Pico Veleta, Spain	2870	1984	30	70	400	0.9	laser (theodol.), holography
9. SEST, Sweden / ESO	La Silla, Chile	2400	1987	15	50	300	0.6	theodolite, holography
10. JCMT, Eng./ Neth./ Can.	Mauna Kea, Hawaii	4000	1987	15	45 35*	330 430*	0.42 0.36	laser, holography
11. CSO, Caltech Sub-mm Obs.	Mauna Kea, Hawaii	4000	1987	10.4	50 20*	210 520	0.6 0.2	laser (distances) holography
12. IRAM, Grenoble	Plateau de BURE, France	2560	1990	15	60	250	0.8	theodolite, holography*
13. SMT, MPIfR / Univ. of Arizona	Mt. Graham, AZ, USA	3250	1991	10	16*	590	0.2	holography*
14. BIMA, Univ. California, Illinois, Maryland	Hatt Creek, MA, USA	1100	1991?	6	17*	350	?	template, holography
15. SMA, Sub-MM Array, SAO	?	?	1995?	6	15*	400	0.35	laser (angles), holography
16. FIRST, ESA	Space (-platform)		2000?	4.5	6*	750	0.1	not yet decided
17. MMA, MM Array, NRAO	Magdalena Moutain	3400	2000?	8	25*	320	1.	not yet decided
18. IVS, Internat. VLBI Sat.	Space (deployable)		?	20	300*	70	?	not yet decided

D = reflector diameter, RMS = surface error (should be one-way phase error), * = performance goal.

a phased response). Pointing errors and aberrations are deduced from a Zernike phasefront analysis. Compensation schemes on the subreflector position to correctly use an homologous primary are deduced from structural calculation results. These prove reliable within 1.E-3 to 1.E-4 on displacements within elastic limits, adding value to the success obtained with the 30m at Pico Veleta, after the Effelsberg 100m (dm range, project: Hachenberg, ≈1960).

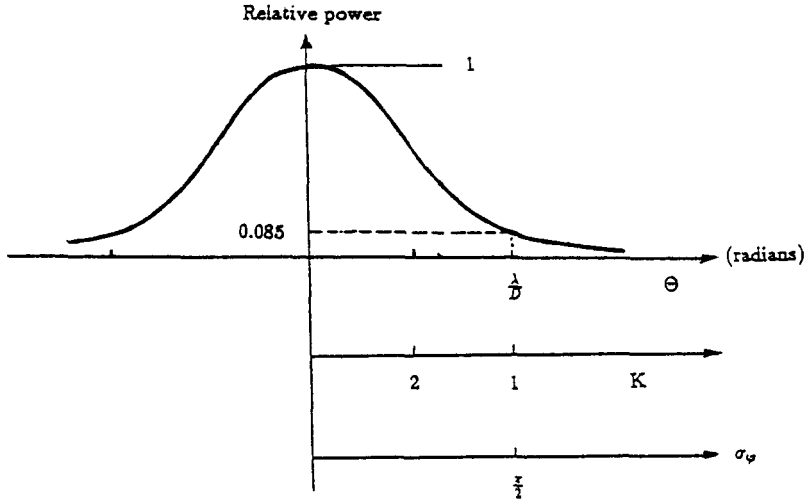

Figure 3: Gaussian approximation of directivity: main beam.

Smaller structures are often quasi-homologous: IRAM recent structural calculations of the ONSALA 20m showed peak errors of 300μ; the 10m Leighton (1978: 3 for OVRO; 1 for CSO in HAWAII; 1 copy at BANGALORE) are lightweight and stiff enough to yield better than 20μ rms computed surface error between 15 and 70 degrees El, in a model based on holographic measurements from 40 to 70 degrees (Woody 1988); the BIMA (Berkeley, Illinois, Maryland Universities) 6m antennas at HAT-CREEK should be corrected for residual coma (Welch 1990: 17μ rms left) by computed subreflector translation. Problems come with size (Von Hoerner 1967): the 70m aerial now erected in conjunction with the "Radio-Astron" project in the USSR should be calculated for partial homology at 3mm waves -it is the last, under construction in Uzbekistan, of a series of 3 distant 70m antennas for space links (Polyak, Bervalds 1990).

MISCELLANEOUS TRENDS: f/D, off-axis, coatings, mounts

Compact constructions are easily stiff, accuracy requirements on surfaces favour them. Their small inertia eases the design of tracking servos, a domain where state variables models have been tried for faster responses, wider band, with mixed results (IRAM 30m: excess motor's fatigue following small predictor model misadjustments). One ends with short primary f/D designs, from 0.50 to 0.25. With large enough magnification M on subreflector, the Nasmyth or Cassegrain combinations do not exhibit more aberrations than their equivalent

https://doi.org/10.1017/S0252921100013002 Published online by Cambridge University Press

long F/D system with $F = Mf$. But the subreflector has to be axially positionned with an absolute accuracy of order $0.3\lambda(f/D)^2$, (WR 205) with edge taper 12dB; and with similar accuracy along a perpendicular direction, to maintain a null dominant coma. Practical limits of 30 to 15μ (1 to 0.5 mm λ) mean f/D =0.3; this is quite general: compact systems are limited by the increase in aberration if very tight constraints in alignment are not fulfilled. The "corrected surface" scheme (e.g. VLA aerials) giving constant illumination on the primary surface to maximize on-axis gain (but enlarging secondary lobes) also boosts the off-axis aberration increase (Napier 1983), considerably reducing the usable FOV ("Field Of View") then multi-beam capability. For space applications, JPL proposes schemes with 2 shaped mirrors near focus to uniformly illuminate a circular aperture from a Gaussian launcher; we experimented at IRAM a single aspherical corrugated teflon lens at the 30m for the same purpose. All these tricks apply for a single receiver aimed at a single direction in space. Shaped surfaces are in use not only at VLA, but also on the 10 VLBA 25m antennas network (NRAO 1987; Thompson 1990). These, as the Australia Telescope antennas (Norris 1987: 7mm and even 3mm prospects), are aimed at dm/cm operation up to 40 GHz, then tested at higher frequencies: a 18% beam efficiency at 86 GHz is reported on a VLBA antenna. This is from surface errors, because shaping gives a frequency independant phasefront on axis; aberrations are reinforced at distance r from axis in the FOV by their natural scaling in r/λ, important at mm frequencies. As conclusion: from the point of view of aberrations and FOV, practical limits to short f/D and compact structures exist in the range currently used.

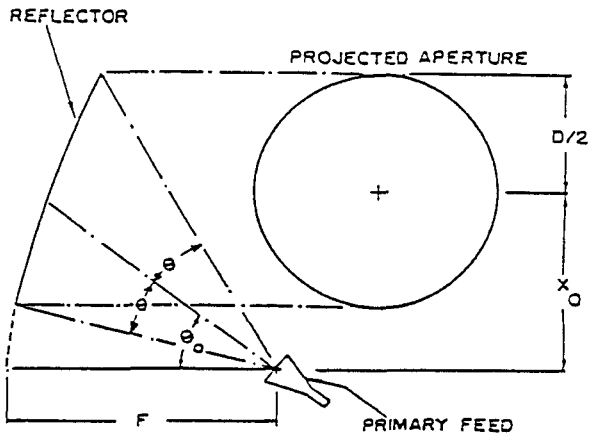

Figure 4: Single reflector off-axis configuration.
In dual reflectors, subreflector and feed replacing primary feed are fully aside of main beam, either in Cassegrain, or Gregorian arrangement.

Spill-over radiation comes in Cassegrain designs mainly from cold sky, with non negligible sensitivity advantage over prime focus arrangements: there a 4% spill-over means 12K added to receiver DSB noise, 2 to 4 times more in system noise for line work. Wobbling modulation on spill-over and losses justifies a slight decrease in subreflector size for far-IR work, rather than an increase for better

https://doi.org/10.1017/S0252921100013002 Published online by Cambridge University Press

FOV coverage with part of spill-over radiation from hot ground. To minimize spill-over, the off-axis design for Cassegrain (or Gregorian) subreflector is now very popular in telecommunication: it suppresses subreflector leg's diffraction and blockage of axi-symmetric structures. The Bell Labs 7m CRAWFORD HILL offset antenna seems to be the only mm radiotelescope of this type. A -10dB advantage on distant secondary lobes can be expected in this "clean lobe" technique, with 2 circularly polarised main beams separated on sky by the "beam-squint" Ψ with $\sin\Psi = \lambda \sin\Theta_0/4\pi F$: Θ_0 = mean offset angle from prime focus, F = parent paraboloid focal length (Rudge, Adatia 1978: see fig. 4). Feed design for dual reflectors should match circular polarisations (Ludwig 1973), not depolarized by the offset paraboloid. Support the subreflector high enough to avoid ground spill-over, accept more panel types to configure the edge, explore homology behaviour of asymmetric structures: this seems the price for better noise, null spectral baseline ripple, zero cross-polar properties. These concepts are retained in the GBT project (new 100m Green Bank Telescope), with a 2 decade frequency range and minimum active corrections.

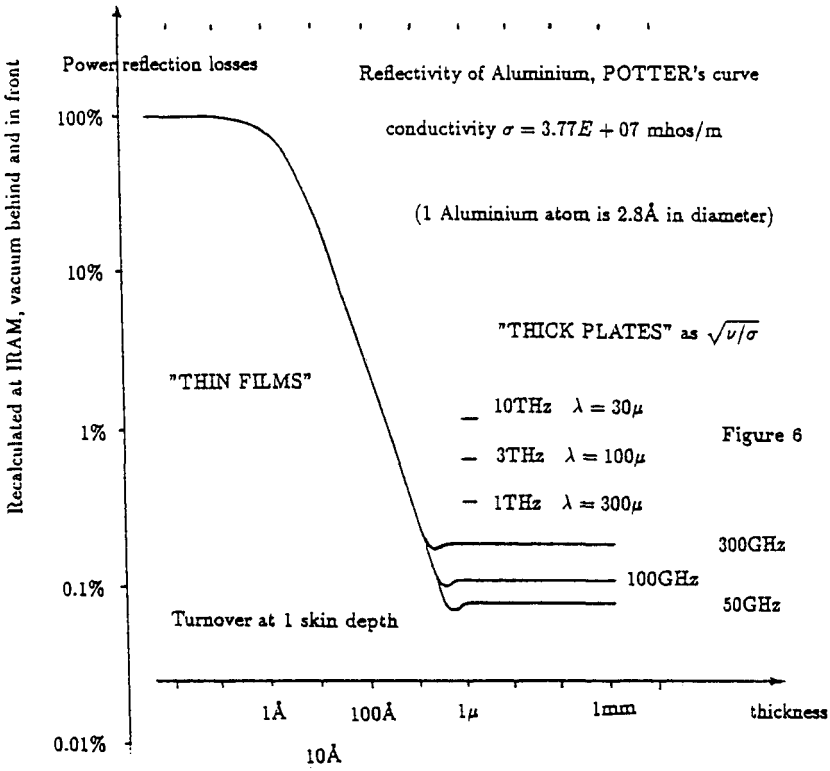

Figure 6

Figure 5: Aluminium reflexion losses vs. thickness of layer.

Surface quality at the λ scale, and surface protection are important in the design. Slope analysis of local roughness was used to predict the near diffuse lobes for the JCMT at HAWAII. The HAT-CREEK solution to diffuse white solar light without impairing mm wave performance is to use milled cast

https://doi.org/10.1017/S0252921100013002 Published online by Cambridge University Press

aluminium alloys panels. With open-air telescopes, low white light absorptivity ϵ_l and medium thermal emissivity ϵ_t prevent thermal gradients under sun by day, or cold sky radiative cooling at night. Plastic film protections should be found with less sub-mm losses than the widely used TiO2 loaded white paint. Excellent by day, this has dew and icing problems at night. IRAM experiments on its 15m and SEST a protective "hostaflon" film (saturated CF_2Cl_2 polymer, mm loss as with teflon, $\epsilon_t \approx 0.5$) on panel's surface. The mm reflector is vacuum deposited aluminium underneath, $\approx$400Å thick, with 1.0% computed (WR 205) reflection loss at 1mm, mainly going to the underlying CFRP (above 1 skin depth i.e. 2μ, this would reduce to 0.1%, see Potter's curve on fig. 5). Intrinsic good surface quality at the λ scale is there, but also: few years lifetime in severe climates, dew and icing protection only eased, and need for a Sun's avoidance zone (30 degrees radius at BURE). Will other long-lived coatings be found in the future with small mm absorption, large corrosion and mechanical resistances, good thermo-optical ϵ_l and ϵ_t ?

Mount construction, drives and servos design are dominated by the pointing accuracy requests. Computers have definitely rendered obsolete equatorial designs; they calculate real-time corrections to any imperfect alignment in alt-az mounts now widely in use, thus putting emphasis on the stability of the mount rather than on its astronomical alignment. Pointing codes based on the IAU J2000 referentials and formulas (Lieske 1977 1979) certainly help when a fraction or an arc-second is needed, with e.g. terrestrial tides in the play. They should be definitely recommended in current radio-astronomical work rather than the more confusing widely used 1950.0 coordinates, enabling for instance new studies of source proper motions, experimental interconnections between referentials, using a good terrestrial rotation model. Very accurate VLBI processing indicates where is the trend (Sovers, Fanselow 1986). Thermal protection is as important as stable mechanical design. The astrodome or radome is a solution for medium or small size installations, keeping vertical gradients under control. It has been adopted for the SMT project at Mt. GRAHAM, and the CSO at HAWAII: medium-sized telescopes of utmost D/ϵ accuracy, $\geq$5.E+05. No interferometer moves a radome (a phase-error source) with antenna from station to station. The present trend in the "radome or not" question is to favour open-air solutions for large structures (diameter $\geq\approx$25m). Then mount thermal behaviour shows up in pointing, calling for good thermal protection and modelling, great care in all mechanical fabrication processes, construction or alignments, to ensure stability.

MEASUREMENTS AND ADJUSTMENTS: holography

At construction time the zenith looking surface is defined with all corrections (e.g. if homology gives a pure paraboloid at a fixed El, known zenith variations follow structural calculations; or shaped surfaces are desired). It is obtained via standard measurements techniques as theodolite and tape, alternately rotating constant angle prisms and modulated light beams to measure distances. Curvature based double integration methods with carts, or spherometers, are efficient on continuous (small) surfaces; templates or rotating arms (used at CRAWFORD-HILL, 12m KITT-PEAK) seem not favoured in setting large antennas. A reference reproduceability is in question, even with alignment laser beams. The Leighton measurement of pathlength from a liquid

https://doi.org/10.1017/S0252921100013002 Published online by Cambridge University Press

surface to focus with a range-measuring laser is reproduceable to 2μ, in a zenith looking laboratory set-up only. Some modal analysis of individual panels deformation was made there, with curvature corrections by loaded springs.

Active ("adaptative" for real time only) control of the emission phasefront consists in measuring phase deviations from a reference plane, then correcting them by surface adjustments (the most natural reference is the received plane wave from a distant point source in an homogeneous enough atmosphere). In holographic measurements, the far-field pattern is measured with phases given by a reference antenna, then Fourier transformed to obtain the aperture complex map. Correlation receivers are ideally suited here. The signal to noise needed when aiming at K independant elements over one aperture diameter -map K by K adjacent beams near focus- is reachable using the total integration time τ available for interferometry between one resolved element and the reference antenna (when scanning a few hours, the information from each element is multiplexed, then Fourier recovered). If $\Delta\nu$ is bandwith, S_f source flux, A equivalent collecting area, η aperture efficiency, T_{sys} equivalent system noise, k Boltzmann constant, the 1σ error $\Delta\epsilon$ on phase-path is, for R at maximum signal on boresight (or R' computed with total area):

$$R = \frac{S}{N} = \eta_c \eta_i \eta_a \sqrt{2\tau\Delta\nu}\,\frac{\eta A S_f}{2kT_{sys}} \qquad \text{then} \qquad \Delta\epsilon = \frac{\lambda}{4\pi}\cdot\frac{1}{R} \qquad \left(\frac{\lambda}{4\pi}\cdot\frac{K}{R'}\right)$$

with under η's the efficiencies for correlator system (e.g. quantization noise), instrument (local oscillator jitter), atmosphere (same, an $\exp(-\sigma_\varphi^2/2)$ formally). This clear result was known from Scott & Ryle (1977). In 1982, D.Morris at IRAM showed that it is possible to associate a phase distribution to the measured amplitude distribution in the focal plane -the so called point-spread function, measured over K beams with sufficient dynamical range- by taking into account a second amplitude distribution in some out-of-focus plane (known defocus amount). An iterative (Misel) algorithm inspired from 3D cristallography is used, with however signal to noise degradation. A lower limit (worst cases) of the minimum signal required corresponds to an $R = S/N$ ratio which is the square of the value derived from above equations (Morris 1982): R values of 50 to 75 dB are often quoted. The Misel iteration gives possible solutions and must be checked for uniform convergence versus various initial conditions. Reconstructing telescopes surfaces and aberrations from only one focal "point spread function" actually needs twice more information. Space beacons can give higher signal to noise and resolution on dish than radiosources in this "phase-retrieval" holography of reflectors. Although the reference surface is plane for a remote source, near emitters have been used (JCMT: Hills, Lasenby 1988) with spherical wave corrections included. At SEST, phase retrieval holography on the 38 GHz signal from LES 8 geostationnary satellite permitted surface adjustment to 55μ rms, with 46% aperture efficiency at 230 GHz.

Motorized actuators, remotely controlled from computer, are used for reproduceability and speed of adjustments with either differential control at SEST and IRAM 15m or a datum point at JCMT (typical readouts -one to few μ- allow setting within about 10μ); modal analysis of panels deformations is part of measurements and adjustment schemes. One distorts panels from their supports to correct piston, tilts, twist defects. Panel structure, homology departures may limit this technique. Corrections from supports is also part of

https://doi.org/10.1017/S0252921100013002 Published online by Cambridge University Press

the adjustment at the IRAM 30m (large enough panels, 18 supports each from a subframe), and the NOBEYAMA antennas.

REFERENCES

DELANNOY, J. 1985, *Proc. of ESO-IRAM-ONSALA Workshop*, Aspenas, p.25-50, ed. ESO, Munchen
HILLS, R., LASENBY, A. 1988, *Cambridge Annual Report*, JCMT
IRAM, *Internal Working Reports: WR*, availalable on request by nr. (or title list) to the librarian, IRAM, Grenoble
LEIGHTON, R.B. 1978, *NSF Grant AST 73-04908 Final Technical Report*, ed. Cal. Tech.
LIESKE, J.H. et al. 1977, *Astr. Ap.*, , **58**, p. 1-16.
LIESKE, J.H. 1979, *Astr. Ap.*, , **73**, p. 282-284; see also *The Astronomical Almanac 1984*, for nutation and others
LUDWIG, A.C. 1973, *IEEE A.P.*, **21**, p. 116-119
MARTIN, R.N., BAARS, J.W.M. 1990, *Proc. of SPIE Conf.* **1236** *on Advanced Technology Optical Telescopes*, The SMT project, Tucson
MASON, C. July 1990, *SMA Documents List (Technical Memos)* and private communication
MORRIS, D. October 1982, *IRAM internal report*, Phase retrieval in the holography of Radio-Reflectors, Grenoble
NAPIER, P. 1983, private communication, NRAO
NORRIS, R.P. 1987, *IAU Symp.* **129**, The Australia Telescope Long Baseline Array, Cambridge, Mass.
NRAO July 1990, *Proposal from Associated Universities to NSF*, The Millimeter Array
NRAO 1987, *IAU Symp.* **129**, The Very Long Baseline Array, Cambridge, Mass.
POLYAK, V.S., BERVALDS, E.Ya. 1990, *Precision Construction of Reflector Radiotelescopes*, Riga (not yet translated from Russian).
RUDGE, A.W., ADATIA, N.A. 1978, *Proc. IEEE* **66**, p. 1592-1619: Offset Parabolic Reflector Antennas, a Review
RUZE, J. 1966, *Proc. IEEE* **54**, p. 633-640, Antenna Tolerance Theory - A Review
SCOTT, P.F., RYLE, M. 1977, *M.N.R.A.S.*, **178**, p. 539-545
SOVERS, O.J., FANSELOW, J.L. 1986, *JPL Publication* **83-39** *Rev. 2*, Observation Model for the VLBI Parameter Estimation Software "MASTERFIT"
THOMPSON, A.R. 1990, *NRAO doc.* **85-13**, and private communication
U.C., Cal.Tech. 1985, *KECK Observatory report* **90**, The design of the KECK Observatory and Telescope; also, 1988: *ESO Conference on very large telescopes*, ed. M.H. Ulrich, ESO, Munchen
Von HOERNER, S. 1967, *Astr. J.* **72**, p. 35-47
WELCH, J. 1990, private communication
WOODY, D. Oct. 1988, *Symp. on MM and Sub-MM Astronomy*, Gravitational Deflection of the Leighton Telescopes, Kona, Hawaii

Toshi Takano: You showed a figure of the surface degradation by wind. What was the wind speed? And are these measured or calculated values?
J. Delannoy : All are calculated values – here for a mean wind speed of 14 m/s). Measurements done up to now at 3cm wavelength have proven that we start to see wind effects (pointing and/or structural) between 10 and 12 m/s mean speed.

P. J. Napier: Why do the temperature gradients across the antennas not decay to zero at night.
J. Delannoy: The hot ground radiation to sky goes through the rear cladding (low time constant there) with anodized aluminum surfaces, then traverses the front panels in reverse sense compared to solar radiation by day. Fluxes are opposite in sign, but about 5 times lower by night.

J. Uson: You showed in one viewgraph a pointing error for the IRAM telescopes of 1"-2". I assume that is at present a goal, but how close are you now to it?
Delannoy: We are a factor of about 2 beyond these specs in "blind pointing" – RMS is 2" to 4" on optical or radio pointing sessions (80 stars, or 30 sources over half the sky). Progress intended now is using inclinometers in quasi real time. (Working at 3mm is no problem; but could be at 1mm.)

https://doi.org/10.1017/S0252921100013002 Published online by Cambridge University Press